

High-fidelity simulation of atomization in diesel engine sprays

By L. Bravo[†], C. B. Ivey, D. Kim[‡] AND S. T. Bose[‡]

A high-fidelity numerical simulation of jet breakup and spray formation from a complex diesel fuel injector has been performed. A full understanding of the primary atomization process of diesel fuel injection has not been achieved for several reasons, including the difficulties in accessing the optically dense region. Due to recent advances in numerical methods and computing resources, high-fidelity simulations of realistic atomizing flows are currently feasible, providing a new mechanism to study the jet breakdown process. In the present study, a novel volume-of-fluid (VOF) method coupled to a stochastic Lagrangian spray (LSP) model is employed to simulate the atomization process. A common rail fuel injector is modeled by a nozzle geometry provided by the engine combustion network (ECN). The working conditions correspond to a single 90 μm orifice JP-8 fueled injector operating at 90 bar and 373 K and releasing into a 100% nitrogen, 29 bar, 300 K ambient with a $Re_l = 16,071$ and $We_l = 75,334$, placing the liquid jet in the atomization breakup regime. The experimental dataset from Army Research Lab (ARL) is used for validation and the Kelvin-Helmholtz/Rayleigh-Taylor (KH-RT) breakup model (Reitz & Bracco 1979) is used for verification, both in terms of spray angle. Droplet distributions of the simulated spray are provided for future experimental comparisons and secondary atomization simulations using LSP modeling.

1. Introduction

To date, one of the main bottlenecks in engineering spray modeling of combustion systems is an accurate description of the primary atomization process. Several contemporary numerical solvers adopt coarse approximations in the dense region based on injecting nozzle-sized particles subject to Kelvin-Helmholtz-type instabilities coupled with Lagrangian particle-tracking techniques (Som & Aggarwal 2009; Senecal 2012). Significant success has been achieved with these methods; however, they require knowledge of the specific spray process to calibrate the model, making a theoretical investigation impossible. Historically, the advancement of primary atomization models has been hindered by the well-known difficulties in measuring the optically dense spray region. Although experimentalists have had success with modern methods, such as ballistic imaging and x-ray techniques, extraction of full four-dimensional information with sufficient spatial and temporal resolution for a detailed analysis is still unfeasible (Linne *et al.* 2006; Wang *et al.* 2006; Coletti *et al.* 2014).

Remarkable progress has been made in recent years in the development of robust numerical methods for handling interfaces, enabling researchers to perform highly resolved simulations of multiphase flow (Gorokhovski & Herrmann 2008). Desjardins *et al.* 2008 reported on the development of the level set/ghost fluid method utilizing high-order

[†] Vehicle Technology Directorate, Army Research Laboratory

[‡] Cascade Technologies Inc.

schemes to study multiphase flows. The accuracy of the numerical technique was corroborated through several studies, including the atomization of a liquid diesel jet at moderately low Reynolds number, $Re = 3000$. In a related study, Desjardins & Pitsch 2010 conducted detailed numerical simulations of primary atomization for several values of Reynolds and Weber numbers ($2000 < Re < 3000$, $500 < We < 2000$), reporting on velocity statistics across the turbulent jet. More recently, using a refined level-set-grid approach, Herrmann 2011 discussed the impact of finite-grid resolution on the phase interface geometry of the liquid jet core under diesel engine conditions with $Re = 5000$ and with an injection velocity of 100 m/s. In this work, it was reported that turbulence is the driving mechanism of atomization within the first 20 diameters downstream of the injector. It was also determined that 6 grid points are needed to obtain grid-independence of large-scale drops. These studies provide a critical database to drive the next-generation spray model development. Note that, as with most other studies, no quantitative comparison to experimental data is typically provided.

The need to accurately model two-phase atomizing flows in high-speed jets is particularly important in diesel injectors where the quality of the fuel and oxidizer mixing is essential for lean combustion. Fuel/air mixture formation is also a very important factor in increasing engine efficiencies and power densities. Spray and atomization characteristics have to be considered to optimize the design of the combustion chamber to reduce exhaust emissions and to improve combustion performance. Also, diesel spray characteristics can be influenced by the injector geometry, the injection parameters, and the flow mixing inside the combustion chamber. Therefore, simulations should account for system-level complexities, including real injector features to accurately predict realistic spray dynamics.

The computational expense of resolving all the critical length scales at large Weber numbers is prohibitively high, so the number of detailed numerical simulations conducted at realistic diesel injector conditions has been severely limited. A liquid jet moving with an $\mathcal{O}(100)$ m/s relative velocity with respect to the quiescent gas can generate droplets with diameters as small as a few microns (Desjardins & Pitsch 2010). Hence, more accurate engineering breakup spray models for the primary and secondary breakup modes are needed to reduce the computational cost when simulating a spray-filled domain.

The objective of the current work is to investigate the atomization behavior of a high-speed single-hole jet with complex internal geometry. A novel unstructured volume-of-fluid (VOF) method has been adopted, which is geometric and unsplit, enforcing exact mass conservation on an unstructured grid (Kim *et al.* 2013, 2014). In this study, the VOF method is coupled to the Lagrangian spray (LSP) framework to increase the computational efficiency and to apply subgrid atomization models. Hence, the phase interface resolved by the grid is captured by the VOF method, while the underresolved small-scale droplets are transferred from the VOF interface representation to the LSP particle tracking, and further breakup is handled by a stochastic breakup model. Measurements were conducted at the Spray and Combustion Research Facility of the Army Research Lab (ARL) to qualitatively complement the simulation and validate spray angle in the simulation. The Kelvin-Helmholtz/Rayleigh-Taylor (KH-RT) breakup model (Reitz & Bracco 1979) is used to further verify the spray angle in the simulation. Droplet distributions were generated for future experimental comparisons and secondary atomization models.

2. Methods

2.1. Simulation

The detailed numerical simulation of the interface was performed using a novel geometric unsplit VOF method that is conservative on unstructured meshes coupled to a stochastic LSP framework. The geometric VOF method ensures discrete conservation and boundedness of the volume fraction, F , by utilizing non-overlapping flux polyhedra for donor volumes (see Ivey & Moin 2012 for a description of flux polyhedra). The VOF method uses piecewise linear interface calculation (PLIC) representation of the interface, requiring an interface normal, \hat{n} . \hat{n} is calculated from an auxiliary level set, G , that was updated using the geometric advection algorithm to keep it consistent with F . Curvature, κ , is also calculated from the G using the direct front curvature method (Herrmann 2006). After \hat{n} and κ are calculated, G is reconstructed to strictly follow the PLIC representation using a bisection algorithm to calculate the local G field (to enforce F) and the reconstructed distance function (Cummins *et al.* 2005) method to propagate the G field throughout the band. For consistency (and stability), mass and momentum are convected using the geometric VOF method. To diminish the strict overflow time-step requirements on VOF schemes, multiple frozen velocity advection updates (taken as 3 here) are performed for each momentum step. Several validation studies have been performed that tested the numerical accuracy and robustness of the solver (Kim *et al.* 2013, 2014).

For computational efficiency, the VOF representation is coupled to a stochastic LSP representation. Interfacial features are characterized by contiguous regions of $F > 0$. Underresolved interfacial flow structures (represented by $< 5^3$ contiguous cells here) are replaced by a spherical droplet of equal volume. No additional breakup model is employed here so as to capture the instabilities leading to atomization directly. LSP droplets follow particle drag laws and a stochastic breakup model based on a critical Webber number (Ham *et al.* 2003).

The simulation was conducted on the nozzle geometry available through the engine combustion network (ECN) with flow conditions corresponding to an injection pressure of 90 bar, a background pressure of 20 bar, and a bulk jet exit velocity of 127 m/s. The Reynolds and Weber numbers were calculated with JP-8 fuel properties database (at 373 K) and yielded a value of $Re_l = 16,071$ and $We_l = 75,334$. The pertinent length scales, determined from the problem configuration, range from the nozzle orifice integral scale ($l_i = d = 90 \mu\text{m}$) to the viscous scale ($0.09 \mu\text{m}$), and down to the Kolmogorov critical radius ($0.2 \mu\text{m}$). The pipe flow viscous scale and the critical radius are defined as

$$l_v = 5.0Re^{-7/8} \quad \text{and} \quad l_{cr} = \left(\frac{\sigma^3}{\rho^3 \epsilon^2} \right)^{1/5}.$$

A large-eddy simulation with a dynamic Smagorinsky model was adopted to treat the smallest flow structures and for computational efficiency. In the nozzle, a wall-resolved approach was utilized with $\Delta x^+, \Delta y^+ \sim 1$ near the wall (calculated from l_v), $\Delta x^+, \Delta y^+ \sim 50$ near the center, and $\Delta z^+ \sim 70$ (see Figure 1). The mesh refinement is cartesian in nature, forcing $\Delta x = \Delta y = \Delta r$. A mesh of ~ 60 million hexahedral control volumes was used to discretize the domain. Mesh points were concentrated in the jet spray envelope to resolve the interface, while coarse buffer regions were added in the radial and axial regions in order to reduce the impact of the boundary conditions (see Figure 2). Within the spray envelope, $\Delta/l_{cr} \sim 0.5$ near the unperturbed nominal interface to capture the instabilities and $\Delta/l_{cr} \sim 40$ throughout the rest of the spray envelope to leverage the LSP framework for savings. The numerical boundary conditions in the ambient region

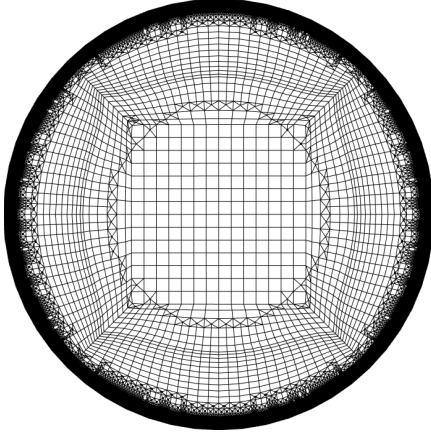


FIGURE 1. Mesh slice at nozzle exit.

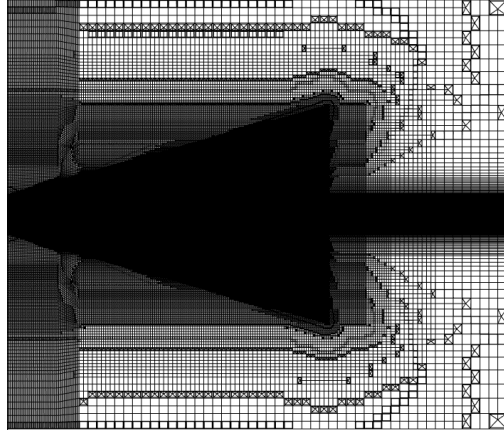


FIGURE 2. Mesh slice through jet centerline.

were a constant inflow set to 5% of the bulk jet velocity, a slip condition over the radial boundaries, and a uniform outflow.

2.2. Experiment

The experiments in this study were conducted at the Army Research Laboratory by injecting a high-speed JP-8 fueled spray into a high-temperature pressure (HTPV) flow-through chamber. The HTPV is designed to reach a maximum pressure of 150 bar and a maximum temperature of 1000 K using a common rail injection system for precise fuel delivery (Kurmann *et al.* 2014). The vessel is equipped with closed loop control for pressure and temperature. The flow-through chamber is held constant at 58 m³/hr. An on-site nitrogen generator produced the necessary nitrogen for testing, which was maintained at 99% purity during experiments. To allow for optical access, the vessel is outfitted with 3 fused silica windows with dimensions of 147 mm diameter by 85 mm thickness. To protect the 85 mm thick pressure windows from fuel contamination, 6 mm thick fused silica windows are placed between the 85 mm windows and the spray zone.

High-speed near-field spray region images were acquired using a single LED light source and a Photron SA5 camera operating at 90,000 fps for line-of-sight measurements. For the experiments presented, image size was set to 320 by 192 pixels and the corresponding scaling was 5.6 μm/pixel. Chamber conditions were set to 20 bar and 300K prescribing a density ratio of 34. Fuel injection pressure was set to 90 bar with a 3 ms injection duration, and a total of 2.2 mg of injected mass was measured via an IAV injection analyzer. Figures 3 and 4 show two instances where the spray behavior goes from transitional to fully atomizing mode.

2.3. Theory

The Reitz dispersion model has been proposed to study the spray angle by employing aerodynamic arguments (Reitz & Bracco 1979). It includes the ratio of the Reynolds and Weber number of the liquid flow in the function $f(\gamma)$ and it is written as

$$\tan(\theta) = \frac{4\pi}{A} \left(\frac{\rho_g}{\rho_l} \right) f(\gamma),$$

where ρ_g and ρ_l are the liquid and gas density, and A is a constant that depends on the nozzle design, $A = 3.0 + 0.28l_0/d_0$, with d_0 is the nozzle diameter and l_0 is the

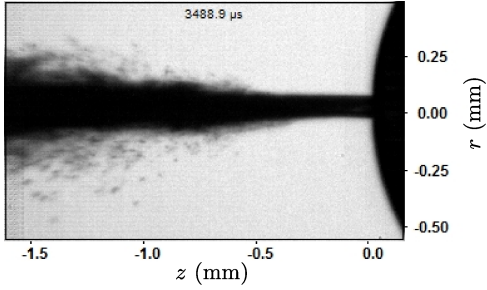


FIGURE 3. High-speed near-field image of JP-8 spray during transition state

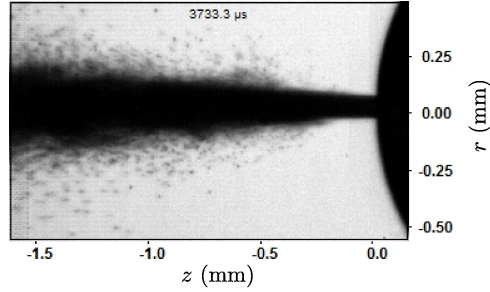


FIGURE 4. High-speed near-field image of JP-8 spray during fully atomized state



FIGURE 5. Q criterion isosurface shaded by streamwise velocity at the bottom wall of the diesel spray injector as viewed from downstream.

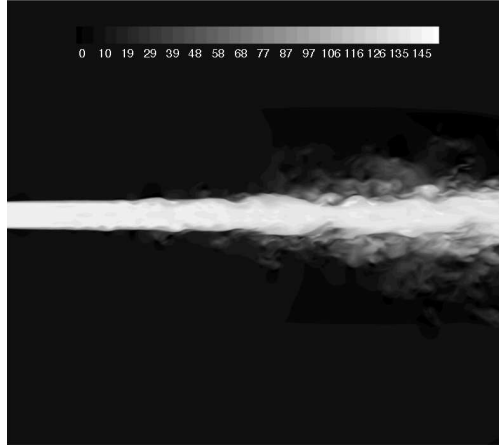


FIGURE 6. Streamwise velocity (m/s) contour over slice at jet centerline.

length of the nozzle hole. The parameter $f(\gamma)$ is a function of the physical properties of the liquid and injection velocity and is defined as $f(\gamma) = \sqrt{3}/6[1 - \exp(-10\gamma)]$ with $\gamma = (\text{Re}_l/\text{We}_l)^2 \rho_l/\rho_g$.

3. Results

The nozzle flow turbulence was visualized by sampling the velocity flow field and using the classical Q criterion defined as $Q = 1/2(\|\Omega_{ij}\| - \|S_{ij}\|)$ and shaded by the streamwise velocity component, U (see Figure 5). The Q criterion isosurface shows hairpin vortex structures arising from the interaction of the fluid with the wall, having peak streamwise velocity magnitudes towards the center of the pipe flow. The vortex structures are irregular as compared to a traditional pipe flow; this discrepancy can be explained by the favorable pressure gradient of the nozzle and the lack of perfect symmetry in the experimentally modeled geometry. Nevertheless, the emerging flow field can be characterized as turbulent, and the resultant jet breakdown can be interpreted as being in the spray atomization regime. The turbulent inflow combined with the jet instabilities lead to the chaotic jet behavior illustrated by the streamwise velocity contour in Figure 6.



FIGURE 7. Volume fraction isosurface and Lagrangian particles alongside the diesel spray injector.

Figure 7 shows the spray formation process at steady full atomization conditions as visualized using the $F = 0.5$ isosurface and the LSP tracked droplets with reference to the nozzle geometry. Note the growth of the hydrodynamic instabilities and the resultant spray cone. The present simulation only models the static fully opened valve configuration.

Figures 8-11 show the radial variations of mean velocity, \overline{U} , and mean volume fraction, \overline{F} , statistics with axial distance. Figure 8 shows the use of 5% co-flow field used to stabilize the solution ($\overline{U} \neq 0$ for $r > D/2$) and the experimental bulk velocity (at $0 D$). Indicative of growing jets, the \overline{U} profiles broaden downstream. Figure 9 shows the \overline{F} distribution, which includes the equivalent volume fraction of the Lagrangian particles. As in \overline{U} , but to a smaller degree, \overline{F} profiles broaden downstream. The \overline{F} profiles decrease in height downstream, demonstrating the breakdown and fluctuation of the liquid jet. Note that the dispersion characteristics between velocity and volume fraction fields are quite different, demonstrating the entrainment effect on the velocity fields and the conservation of mass of the volume fraction fields. The turbulent kinetic energy (TKE) radial profiles are shown in Figure 10. The nozzle pipe flow injects sharp TKE peaks, generating turbulent structures at fluid interface. The TKE facilitates the jet breakdown and grows with the

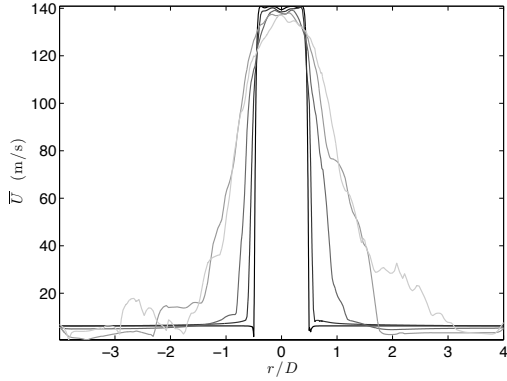


FIGURE 8. Mean streamwise velocity as a function of radial distance for 5 downstream stations: $z/D = \{0, 4, 8, 12, 16\}$ (dark to light).

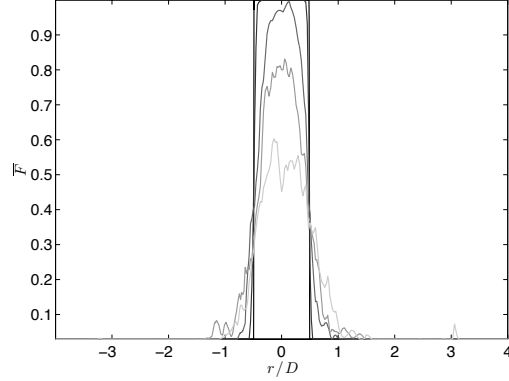


FIGURE 9. Mean volume fraction (including Lagrangian spray) as a function of radial distance for 5 downstream stations: $z/D = \{0, 4, 8, 12, 16\}$ (dark to light).

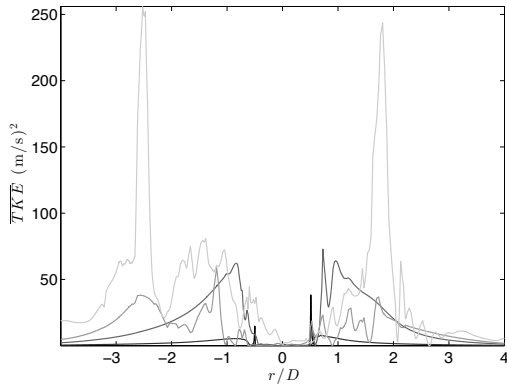


FIGURE 10. Mean turbulent kinetic energy as a function of radial distance for 5 downstream stations: $z/D = \{0, 4, 8, 12, 16\}$ (dark to light).

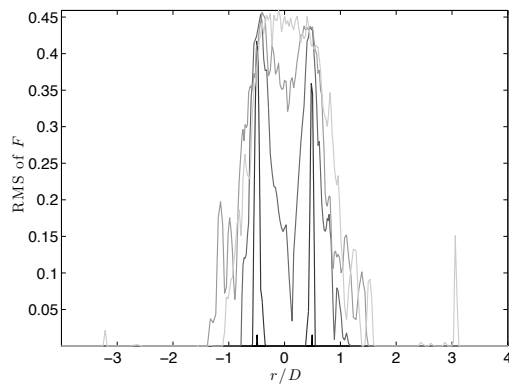


FIGURE 11. Root mean square of volume fraction (including Lagrangian spray) as a function of radial distance for 5 downstream stations: $z/D = \{0, 4, 8, 12, 16\}$ (dark to light).

shear layer. Figure 11 shows the intensity, F root mean square (RMS), profiles spreading with the growth of the shear growth layer.

The statistics have not fully converged, as shown in Figure 8, so in order to extract a preliminary estimate of the spray angle, θ , we fit a Gaussian curve to each of the mean velocity profiles. Figure 12 shows the Gaussian fits, which are not centered at the origin, evidencing the lack of axisymmetry of the real geometry (the spray comes off at an angle). The full-width half-maximum (FWHM) of the Gaussian fits to the mean streamwise profiles is shown in Figure 13; the change of the linear fit to the FWHM with axial distance provides the spray angle, θ .

The experimental spray angle was determined via line-of-sight observations of 200 spray images (sampling frequency of $11.1 \mu\text{s}$) while tracking the interface of the jet core region with respect to the jet centerline. The total sampling time corresponds to 2.2 ms in the full atomization spray mode ($\text{Re} = 16,071$ and $\text{Oh} = 0.017$). The initial transients were not included in the procedure for consistency with the simulation results. The spray

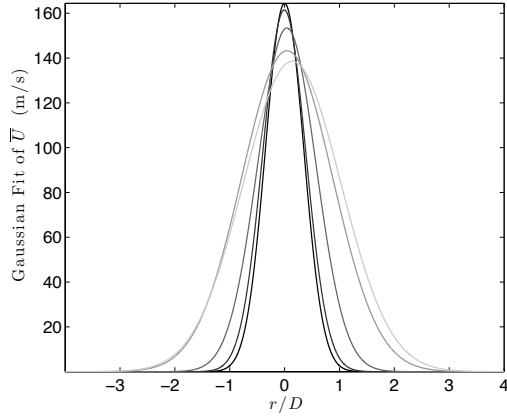


FIGURE 12. Gaussian fit to mean streamwise velocity as a function of radial distance for 5 downstream stations: $z/D = \{0, 4, 8, 12, 16\}$ (dark to light).

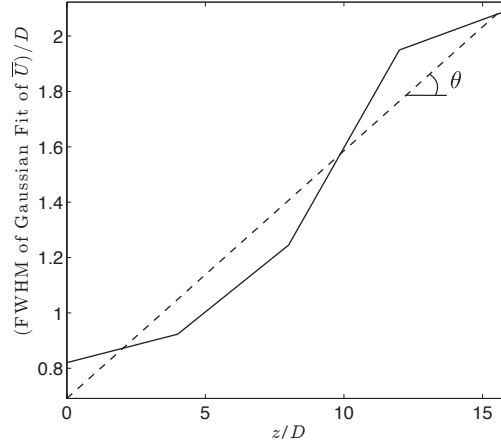


FIGURE 13. Full width half maximum of gaussian fit to mean stream wise velocity as a function of downstream location. θ is the angle of linear fit to the full width half maximum (dashed line).

angles extracted from Reitz theory, simulation, and experiment are, respectively,

$$\theta_{\text{Reitz}} = 5.8^\circ, \quad \theta_{\text{sim}} = 5.1^\circ, \quad \text{and} \quad \theta_{\text{exp}} \sim 4^\circ. \quad (3.1)$$

The simulation and theoretical dispersion results appear to be in good agreement. However, there is a 1° discrepancy with the experiments featuring a spray angle of 4° . The differences can be in part due to variations in the nozzle orifice diameter and nozzle shape that arise from manufacturing fabrication eccentricities and due to cavitation within the nozzle. This discrepancy has been discussed in the literature previously for ECN-type injectors where geometric inconsistencies were thoroughly reported (Kastengran *et al.* 2012). The impact of these discrepancies can clearly affect the spray parameters.

Secondary atomization models require an initial droplet spray profile, parameterized by droplet diameter and distance away from jet. Droplet sizes and counts are calculated from the combination of the LSP particles and the resolved VOF features (calculated using the same method to transfer from VOF to LSP for underresolved features, but with a larger domain cell count). Figure 14 shows the average number of droplets for a given droplet diameter. The droplets range from approximately $1 - 10 \mu\text{m}$, the average droplet diameter is $3.0 \mu\text{m}$, and the most likely droplet diameter is $1.5 \mu\text{m}$. Droplet diameters $< 1 \mu\text{m}$ were spontaneously evaporated and were not tracked. Figure 15 shows the average droplet diameter at a given distance away from the jet center. The average droplet size increases away from the jet, going from approximately $2 - 7 \mu\text{m}$.

4. Conclusions

In this investigation a high-fidelity simulation approach was adopted to study the atomization physics of a diesel injector with detailed nozzle internal geometry. The nozzle flow field was characterized through visualizations of Q isosurfaces for turbulence patterns. The complexity of the geometry and system dynamics was characterized by a snapshot of the volume fraction isosurface and Lagrangian droplets. Also, mean streamwise velocity and volume fraction statistics show the structure of the high-speed jet. The

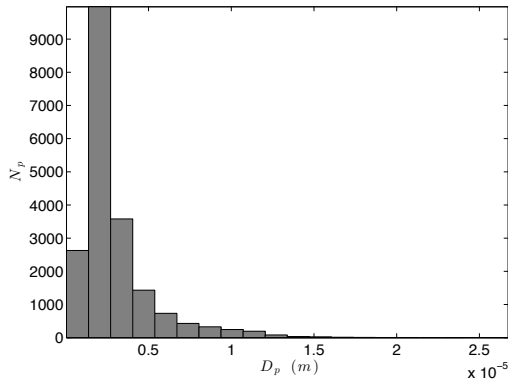


FIGURE 14. Number of droplets as a function of diameter.

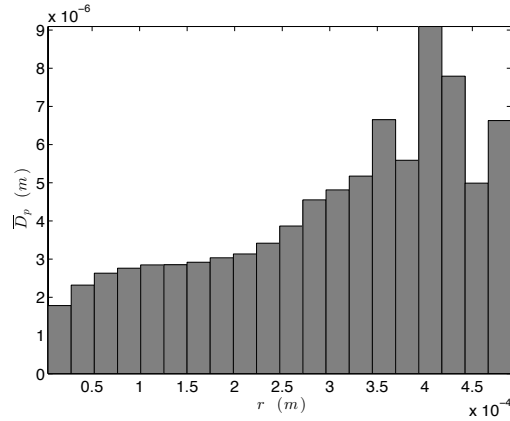


FIGURE 15. Mean droplet diameter as a function of radial distance.

turbulent kinetic energy and volume fraction intensity profiles characterize the interfacial mixing processes. Comparison with Reitz spray theory and ARL measurements of the near nozzle flow field show that the simulation captures the correct dispersion characteristics. The spray was further characterized using droplet size and spatial distribution plots. Further work is presently under way, using higher resolution to establish numerical convergence and to capture the hydrodynamic flow instabilities for comparison with classical instability models.

Acknowledgments

The authors acknowledge use of computational resources from the Certainty cluster awarded by the National Science Foundation to CTR. An award of computer time was provided by the Innovative and Novel Computational Impact on Theory and Experiment (INCITE) program. This research used resources of the Argonne Leadership Computing Facility at Argonne National Laboratory, which is supported by the Office of Science of the U.S. Department of Energy under contract DE-AC02-06CH11357. This research was supported in part by an appointment to Luis Bravo by the U.S. Army Research Laboratory Postdoctoral Fellowship Program administered by the Oak Ridge Associated Universities through a contract with ARL.

REFERENCES

- COLETTI, F., BENSON, M. J., SAGUES, A. L., MILLER, B. H., FAHRIG, R. & EATON, J. K. 2014 Three-dimensional mass fraction distribution of a spray measured by x-ray computed tomography. *J. Eng. Gas Turb. Power* **136**, 051508.
- CUMMINS, S. J., FRANCOIS, M. M. & KOTHE, D. B. 2005 Estimating curvature from volume fractions. *Computers Structures* **83**, 425–434.
- DESJARDINS, O., MOUREAU, V. & PITSCH, H. 2008 An accurate conservative level set/ghost fluid method for simulating turbulent atomization. *J. Comput. Phys.* **227**, 8395–8416.
- DESJARDINS, O. & PITSCH, H. 2010 Detailed numerical investigation of turbulent atomization of liquid jets. *Atomization Sprays* **20**, 311–336.

- GOROKHOVSKI, M. & HERRMANN, M. 2008 Modeling primary atomization. *Ann. Rev. Fluid Mech.* **40**, 343–366.
- HAM, F., APTE, S., IACCARINO, G., WU, X., HERRMANN, M., CONSTANTINESCU, G., MAHESH, K. & MOIN, P. 2003 Unstructured les of reacting multiphase flows in realistic gas turbine combustors. *Annual Research Briefs*, Center for Turbulence Research, Stanford University.
- HERRMANN, M. 2006 A balanced force refined level set grid method for two-phase flows on unstructured flow solver grids. *Annual Research Briefs*, Center for Turbulence Research, Stanford University.
- HERRMANN, M. 2011 On simulating primary atomization using the refined level set grid method. *Atomization Sprays* **21**, 283–301.
- IVEY, C. B. & MOIN, P. 2012 Conservative volume of fluid advection method on unstructured grids in three dimensions. *Annual Research Briefs*, Center for Turbulence Research, Stanford University.
- KASTENGRAN, A. L., TILOCCO, F. Z., DUKE, D. J., MANIN, J., PICKETT, L. M., PAYRI, R. & BAZYN, T. 2012 Engine combustion network (ecn): measurements of nozzle geometry and hydraulic behavior. *Atomization Sprays* **22**, 1011–1052.
- KIM, D., HAM, F., BOSE, S., LE, H., HERRMANN, M., LI, X., SOTERIOU, C. & KIM, W. 2014 High fidelity atomization in a gas turbine injector high shear nozzle. In *Institute for Liquid Atomization and Spray Systems, 26th Annual Conference*.
- KIM, D., MANI, A. & MOIN, P. 2013 Numerical simulation of bubble formation by breaking waves in turbulent two-phase couette flow. *Annual Research Briefs*, Center for Turbulence Research, Stanford University.
- KURMANN, M., BRAVO, L., KWEON, C. B. & TESS, M. 2014 The effect of fuel injector nozzle configuration on jp-8 sprays at diesel engine conditions. In *Institute for Liquid Atomization and Spray Systems, 26th Annual Conference*.
- LINNE, M., PACIARONI, M., HALL, T. & PARKER, T. 2006 Ballistic imaging of the near field in a diesel spray. *Exp. Fluids* **40**, 836–846.
- REITZ, R. D. & BRACCO, F. B. 1979 On the dependence of spray angle and other spray parameters on nozzle design and operating conditions. *SAE Technical Paper* p. 790494.
- SENECAL, P. 2012 Grid convergent spray models for internal combustion engine cfd simulations. In *Proceedings fo the ASME 2012 ICE Division Fall Technical Conference*.
- SOM, S. & AGGARWAL, S. K. 2009 Assessment of atomization models for diesel engine simulations. *Atomization Sprays* **19**, 885–903.
- WANG, Y. J., IM, K. S., FEZZAA, K., LEE, W. K., WANG, J., MICHELI, P. & LAUB, C. 2006 Quantitative x-ray phase contrast imaging of air-assisted water sprays with high weber numbers. *Appl. Phys. Lett.* **89**, 151913.